Air Products

Air Products and Chemicals, Inc.
Box 538, Allentown, PA 18105
(215) 481-4911

8 August 1984

Director, Advanced Research
Projects Agency
1400 Wilson Boulevard
Arlington, VA 22209

Attention: Program Management

Gentlemen:

SUBJECT: Contract	N00014-83-C-0394
Item No. 0002	Data
Sub-Item A001	R&D Status Report #4

Attached is R&D Status Report #4 for the subject contract covering the period from 1 April 1984 to 30 June 1984.

Very truly yours,

Ralph C. Longsworth

Ralph C. Longsworth
Program Manager

sk

cc: Scientific Officer
DCASMA - Reading, Pa.
Director, Naval Research Laboratory
Defense Technical Information Center

Enclosures

Air Products

R&D STATUS REPORT

DARPA ORDER NO.: 4746 PROGRAM CODE NO.: --

CONTRACTOR: Air Products and Chemicals, Inc.

CONTRACT NO.: N00014-83-C-0394 CONTRACT AMOUNT: $594,000

EFFECTIVE DATE OF CONTRACT: '83 July 01

EXPIRATION OF CONTRACT: '84 June 30

PRINCIPAL INVESTIGATOR: W. A. Steyert PHONE NO.: (215) 481-3700

PROGRAM MANAGER: R. C. Longsworth PHONE NO.: (215) 481-3708

SHORT TITLE OF WORK: Solid State Compressor

REPORTING PERIOD: '84 April 01 - '84 June 30

- o PROGRESS:

  Progress Report is attached.

- o KEY PERSONNEL: No changes

- o SPECIAL EVENTS: None

- o PROBLEMS ENCOUNTERED AND/OR ANTICIPATED: None

- o ACTION REQUIRED BY THE GOVERNMENT: None

- o FISCAL STATUS:

  (1) Amount currently provided on contract: $200,000

  (2) Expenditure and commitments to date: Per separate report

  (3) Funds required to complete work: Per contract

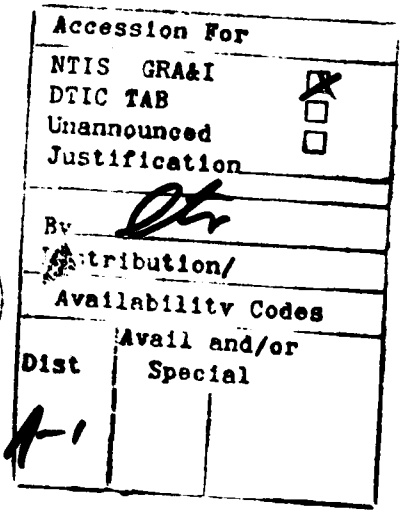

Air Products

1.0 SUMMARY

$Pb(Mg_{1/3}Nb_{2/3})O_3$: 10% $PbTiO_3$ will be used for the first driven ceramics. They will be fabricated in the simpler transverse field geometry. This provides a smaller motion and force than the more favorable longitudinal field geometry, but is easier to implement initially. Two neoprenes, one Monothane, and two special Air Products' polyurethane elastomers, all of low Durometer, were tested in the 0.005 to 62 Hz frequency region and at temperatures varying from 20° to 70°C. The best material found for use as a motion amplifier was the 0 nominal Durometer neoprene; it has a modulus of about 100 psi in the 200 to 1,000 Hz frequency region at room temperature. A one cell compressor unit was built and given a preliminary test using a hydraulic test system. Pumping action was observed. The mechanical design of the three cell simulator has been completed except for the elastomeric compressor components.

Air Products

2.0 TASK 1.1 ELECTROSTRICTION ACTUATORS FOR A SOLID STATE COMPRESSOR

2.1 Design Considerations

Initial Phase

To simplify the initial processing requirements, it was decided to fabricate the first family of ceramic actuators using a composition in the Pb $(Mg_{1/3}Nb_{2/3})\ O_3$:$PbTiO_3$ family of electrostrictors. The reason for this choice is that these materials have been very extensively researched both here at Penn State in MRL, and at the Optics Division of ITEK Corporation in Boston.

The material has been demonstrated to tape cast in a satisfactory manner using a standard Cladan proprietary dispersion system, and electrode inks which are compatible with the tape and binder have been chosen. In the work of S. J. Jang at Penn State, it was shown that the realizable electrostrictive strain increases with $PbTiO_3$ addition to lead magnesium niobate up to a composition of 13 mole% $PbTiO_3$, but at the expense of reproducibility and added hysteresis in the strain. These features are highly undesirable in deformable mirrors, but would be of little consequence in the pump activator.

In spite of the obvious advantage of higher $PbTiO_3$ content, we believe it politic to start with the 10% $PbTiO_3$ composition since all parameters for the tape casting are well defined in this system. As the casting progresses, we intend to move to high $PbTiO_3$ compositions.

Very recent work (April 1984) has indicated that in the transverse mode, lead lanthanum zirconate titanate (PLZT) compositions in the region of the 9.5:65:35 composition have significantly larger strain capability as compared to the PMN:PT system. Here, however, the technology for casting is not yet developed and must be started in parallel with the PMN:PT developments.

Air Products

Design of the Actuator

We propose to fabricate the first actuators using the simpler construction of a transverse field device. In this construction, the electrodes lie parallel to the long axis of the actuator in the monolithic tape cast body. To facilitate firing and avoid warpage during the binder burnout procedure, the actuator will not be constructed from a single run of tape but will be assembled from individual multilayer building blocks.

In the first runs each block will have dimensions 2.5 x 1.25 cm (1" x 1/2") on the larger faces and will be made up from 20 layers of 5 mil thick (fired) tape; electrodes will be screen printed onto the sheets, inset at alternate ends so that alternate fired in electrode sheets can be picked up by the silver end termination.

To assemble the proposed 10 cm long actuator, 4 blocks will be assembled end to end. We will explore co-joining by the termination metallization and/or by solder joining or by Ag epoxy. It is anticipated that each actuator block may be cast with extra outer protective layers, so that after assembly the surfaces may be ground and polished to plane parallel surfaces. To complete the actuator, four element rods can be bonded side by side using epoxy cement to make up the required driver configuration.

Advantages of this mode of construction are:

1. Individual tape cast units are short enough to avoid problems of warping during firing.
2. Individual units can be pretested before fabrication so that elements with short or open circuit plates can be eliminated. Dilation performance of each unit can be checked before the more expensive finishing operations.
3. Termination silvering can be kept very thin so that only thin, stiff metallic links are in series with the high stress direction of the actuator.

4. By using four elements in series, the outermost terminations can be kept at a common ground potential and the design of the cradle to hold the pusher correspondingly simplified.

2.2 Current Status

Initial batches of the PMN:PT did not produce a satisfactory ceramic. Initial test samples fabricated from the powders gave unsatisfactory permittivity and low electrostrictive strain. The problem appears to be associated with the batch of magnesium oxide used in the mixture. To improve the reactivity, new batches of the precursor magnesium niobate have been fabricated using high grade magnesium carbonate as the starting powder.

The new powders fabricate to a ceramic body with properties superior to the original data from Jang and now appear satisfactory for the fabrication of tapes. Slurries are now being prepared using various weight percents of Cladan CB73115 binder system.

As a precaution to avoid any further delays in tape fabrication, a 1 kg lot of PMN:10% PT powder has been ordered from ITEK and experiments will be carried out in parallel between the PSU and ITEK compositions.

Air Products

3.0 TASK 2.1 ONE CELL SIMULATOR

3.1 Design and Construction

Figure 3.1 shows the one cell simulator. An oscillating force exerted by our hydraulic unit (shown in Figure 3.2 of our April 1984 report) on the force plate causes the elastomer to fill the compression space, expelling gas through the outlet check valve. Figure 3.2 shows that a small movement of the force plate results in a much larger motion of the elastomer into the compression space; this is the motion amplification principle.

Figure 3.3 shows the mold that allowed the construction of the force plate elastomer unit. Liquid Monothane* was poured into the mold; then the force plate was placed in the mold. The elastomer was forced out the vent holes. A great deal of care was required to assure that the elastomer was free of air bubbles. We tried to force the bubbles up through the vent holes. It seems that injection molding might be a preferred method for preparing this part, but we are not currently set up for injection molding.

Figure 3.4 shows the compressor head details. This unit was given a preliminary test and did provide gas compression. The next step will be to measure a quantitative pressure buildup and flow rate correlation.

3.2 Dynamic Elastomer Testing

The modulus of elasticity for five elastomers was measured as a function of frequency and temperature. The frequency range covered was 0.005 Hz to 62 Hz; temperatures varied from -20°C to 70°C. Figure 3.5 shows

---

* One-component, castable polyurethane resin marketed by Synair Corporation, Chattanooga, Tennessee.

Air Products

the geometry of the elastomer under test. Figure 3.1 of the April 1984 progress report shows the method used to measure the force, F, and the motion, δ, of the elastomer as the oscillating force is applied.

The modulus of elasticity, E, can be deduced from Eq. 17 of the January 1984 progress report:

$$P = (3/8)d^2 S\delta/w^3 \qquad (1)$$

or

$$(\pi/4)F = (3/8)\ \delta\ (E/3)/w^3 \qquad (2)$$

In Equations 1 and 2 P is the pressure on the force plate ($=(\pi/4)F$ if the plate diameter is 1") and G is the shear modulus = E/3 if the P Poisson's ratio of the elastomer is 1/2 (See Eq. 3 of January, 1984 progress report). Figure 3.5 shows that w is the elastomer thickness.

The five elastomers tested were:

1. Nominal 30 Durometer neoprene (We measured as 40 Durometer; we measured static E as 190 psi)

2. Nominal 10 Durometer Monothane (We measured 11 Durometer, static E is 30 psi)

3. Nominal 0 Durometer neoprene (We measure 20 Durometer, obtained from Valvic, Inc., Three Bridges, New Jersey)

4. Special Air Products Polyurethane Compound 7783-35-3 (Measured as 34 Durometer)

5. Special Air Products Polyurethane Compound 7783-39-1 (Measured as 3 Durometer)

In order to correlate the results at the various temperatures and frequencies, we employ viscoelastic theory, as discussed, for instance in "Viscoelastic Properties of Polymers", J. D. Ferry, John Wiley and Sons, New York, 1961.

Air Products

Figure 3.6 illustrates the correlated results. Viscoelastic theory allows us to extract the expected modulus at frequencies beyond the range of measurement from measurements made at varying temperatures. Some of the details of this method and the Maxwell-Wiechart model were discussed in the April 1984 progress report.

We can see from the figure that the special Air Products' elastomers have a much higher modulus at higher frequencies; their usefulness as elastomeric motion amplifiers in this application would be limited to lower frequency operation. Monothane of 10 Durometer does not seem too bad, but the best materials, at least in regard to a low modulus, are the neoprenes. In the range of 200 to 1,000 Hz where we expect this compressor to operate, the best material tested is 0 Durometer neoprene with a modulus, E, of 70 psi to 140 psi.

Air Products

4.0 TASK 2.2 THREE CELL SIMULATOR, CPI

4.1 Mechanical Design

The purpose of this research is to perform feasibility studies aimed at a solid state, electrostrictive gas compressor. A critical component of this effort is to demonstrate pumping action based on a mechanical simulator, and in this report we document specific designs of a mechical, three cell simulator mechanism developed after several iterations.

The detailed mechanism is shown drawn to scale in Figure 4.1. A motor driven cam activates a cam rod which stresses a molded elastomer via a force member. A chassis is positioned with mounted micrometer heads, and the undercarriage consists of ball bearing mounted brackets riding on a positioned shaft. A compression spring mounted on the cam rod is adjusted to provide at least 10 lbs. of return force via the adjustable cam rod which rides through a ball bearing mount in the spring bracket. A guide rod mounted on the cam rod assembly insures alignment of the cam, and load cells are mounted directly in the drive train. A turnbuckle in the drive train provides linear adjustment.

Figure 4.2 gives an elevation view of the simulator to compliment Figure 4.1 A chassis anchor bracket is shown in Figure 4.2, adjustable in two dimensions. The concept here is that the micrometer heads are used to position the chassis to satisfy zero force on the elastomer at the proper cam positions; next the chassis is anchored via the chassis anchor brackets. The spring bracket is adjustable also to allow positioning of various molded elastomers.

Figure 4.3 shows the details of the motor and shaft mountings. As seen, the motor and bearings have to be mounted above the base plate to satisfy the dimensional requirements in Figures 4.1 and 4.2. A bellows coupling is specified in Figure 4.3 to eliminate misalignment problems, as are the self-aligning bearings in the shaft hangers.

Air Products

4.2 Cam Design

We are aiming for a self-valving design. We design cams on that basis. It seems axiomatic that the three cams involved be identical for the following reasons:

1. The cost of machining the cams is minimized.
2. Spare cams can be easily made.
3. The cams are then nominally interchangeable.

If the number of cams is limited to three, it is a simple exercise to convince oneself that the phase relation between the cams mounted on the motor shaft must be 120°. The completely self-valving feature has much merit in that the overall design is simplified, but--more importantly--the actual operation is more closely simulated.

The problem then reduces to the following: Given a 120° phase relation, what is the optimum dwell angle of the cams for a three cell device? On constructing graphical representations of these relationships, it readily became apparent that a 120° dwell was the minimum dwell angle for self-valving. The 120° phase - 120° dwell case is illustrated in Figures 4.4 and 4.5. Referring to Figure 4.4 it is seen that the outlet cell is valved for $330° < \theta < 90°$ and the inlet cell is valved for $90° < \theta < 210°$. Although this appears reasonable, Figure 4.5 shows that there is only a point overlap between the opening and closing of the critical cells (note the 30° offset between Figures 4.4 and 4.5). For example, referring to Figure 4.4, it is precisely at 210° that both cells #1 and #2 are closed although Figure 4.4 does not readily convey this point. At 330° cells #2 and #3 are closed but only for that instant. Thus, any minute errors in machining or positioning will lead to backstreaming in the 120° phase - 120° dwell case.

The 120° phase - 150° dwell case is illustrated in Figures 4.6 and 4.7. Here there is a "30° overlap" between the opening and closing or critical

cells as shown in Figure 4.7. This appears to be the more reasonable case practically.

Therefore, the concept of a completely self-valving three cell simulator seems practical. However, there is a certain price to be paid here; namely the throughput of the simulator is considerably reduced. This is illustrated in Figure 4.8 which shows the volume of gas compressed per cycle (in arbitrary units) for three cases: (1) the original, semi-self-valved case; (2) the 120° phase - 120° dwell case; and (3) the 120° phase - 150° dwell case. As seen, the throughput for the third case is $\approx$1/3 that of the first case.

Proceeding further, the pressure buildup in a 7-cm diam. surge tank was previously estimated for the semi-self-valved case according to:

$$P_t/P_o = 1 + \omega t(\nu/V) \qquad (1)$$

Adopting the same parameters used previously, we can estimate the pressure buildup for the 120° phase - 150° dwell case, and these estimates are given in Table I.

TABLE I. PRESSURE BUILDUP, THREE CELL SIMULATOR (120° phase, 150° dwell, 7-cm-diam. surge tank, 0.0125 "channel diam., 1" cell length)

	P_t/P_o		
t(hr)	1000 rpm	3000 rpm	5000 rpm
1	1.20	1.60	2.01
2	1.41	2.21	3.02
3	1.60	2.81	4.03
4	1.81	3.42	5.03
5	2.01	4.03	6.03

Air Products

Therefore, although the throughput for the 120° phase - 150° dwell case is considerably reduced, nonetheless the P_t/P_o values in Table I are attractively large and easily measureable for convenient running times.

We conclude, therefore, that the completely self-valved, 120° phase = 150° dwell case is vastly superior to the previous, semi-valved case.

Finally, the defining equations for the 150° - dwell, compressed cycloidal cam for cell #1 are as follows:

$$y = (h/\pi)\ (12\theta/7 - \tfrac{1}{2} \sin 24\theta/7),\ \theta < 105° = 7\pi/12, \tag{2}$$

$$y = h;\ 105° < \theta < 255°$$

$$y' = (12h/7\pi)\ (1 - \cos 24\theta/7),\ \theta < 105°, \tag{3}$$

$$y'' = (288h/49\pi) \sin 24\theta/7,\ \theta < 105°, \tag{4}$$

where h is the maximum lift and y' and y" are the velocities and accelerations of the lift. As discussed previously, there are no discontinuities in the acceleration of the cycloidal cam which could lead to chatter. Equation (2) will be used for the cam design.

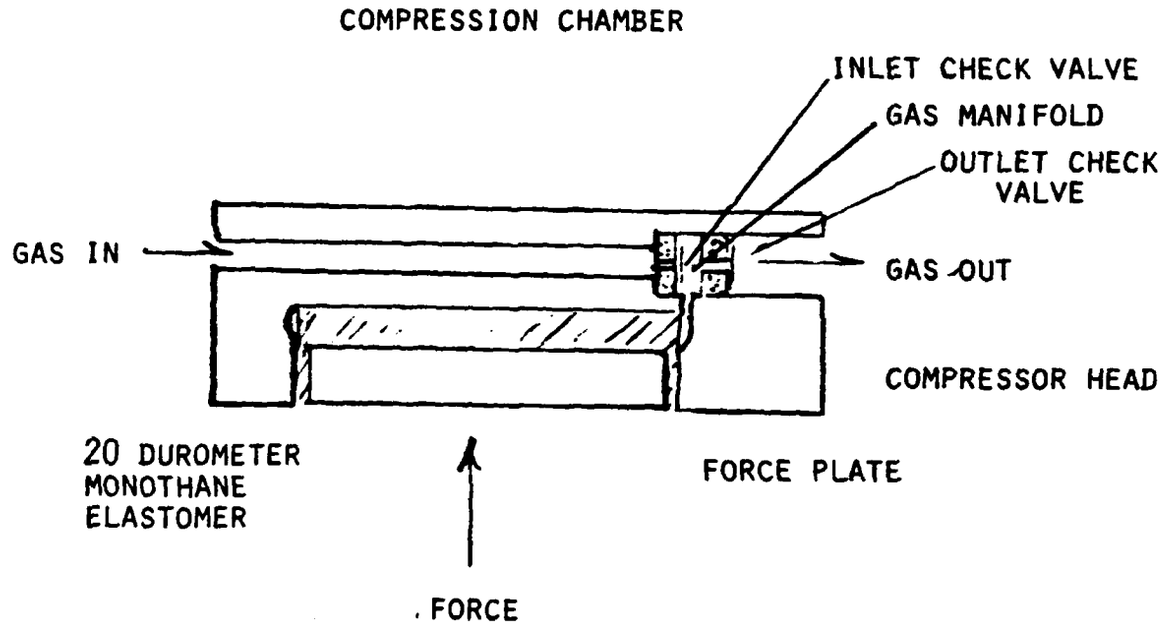

Figure 3.1 One Cell Simulator

Low pressure gas enters through fitting (not shown), enters compression chamber through inlet check valve, and leaves through outlet check valve and fitting (not shown). The gas manifold size is exaggerated for clarity.

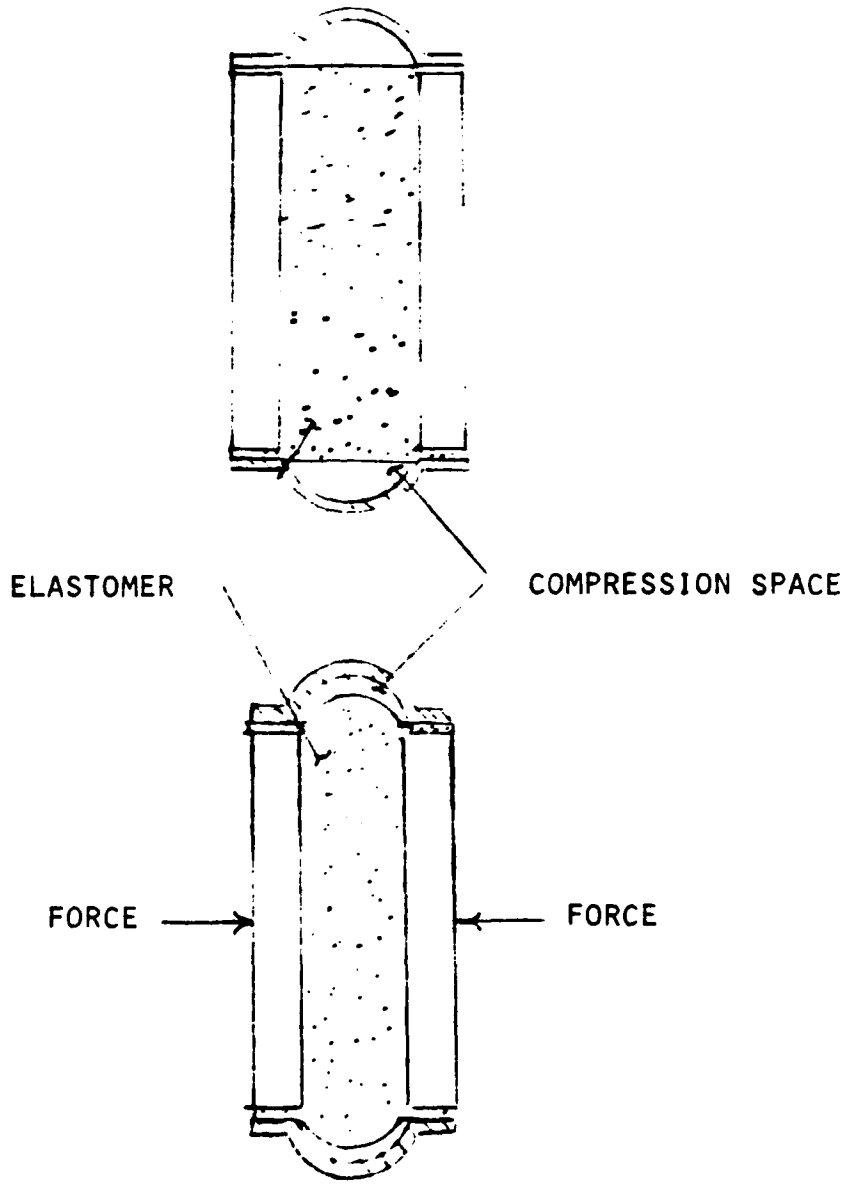

Figure 3.2 Pumping Action Using Elastomeric Motion Amplifier

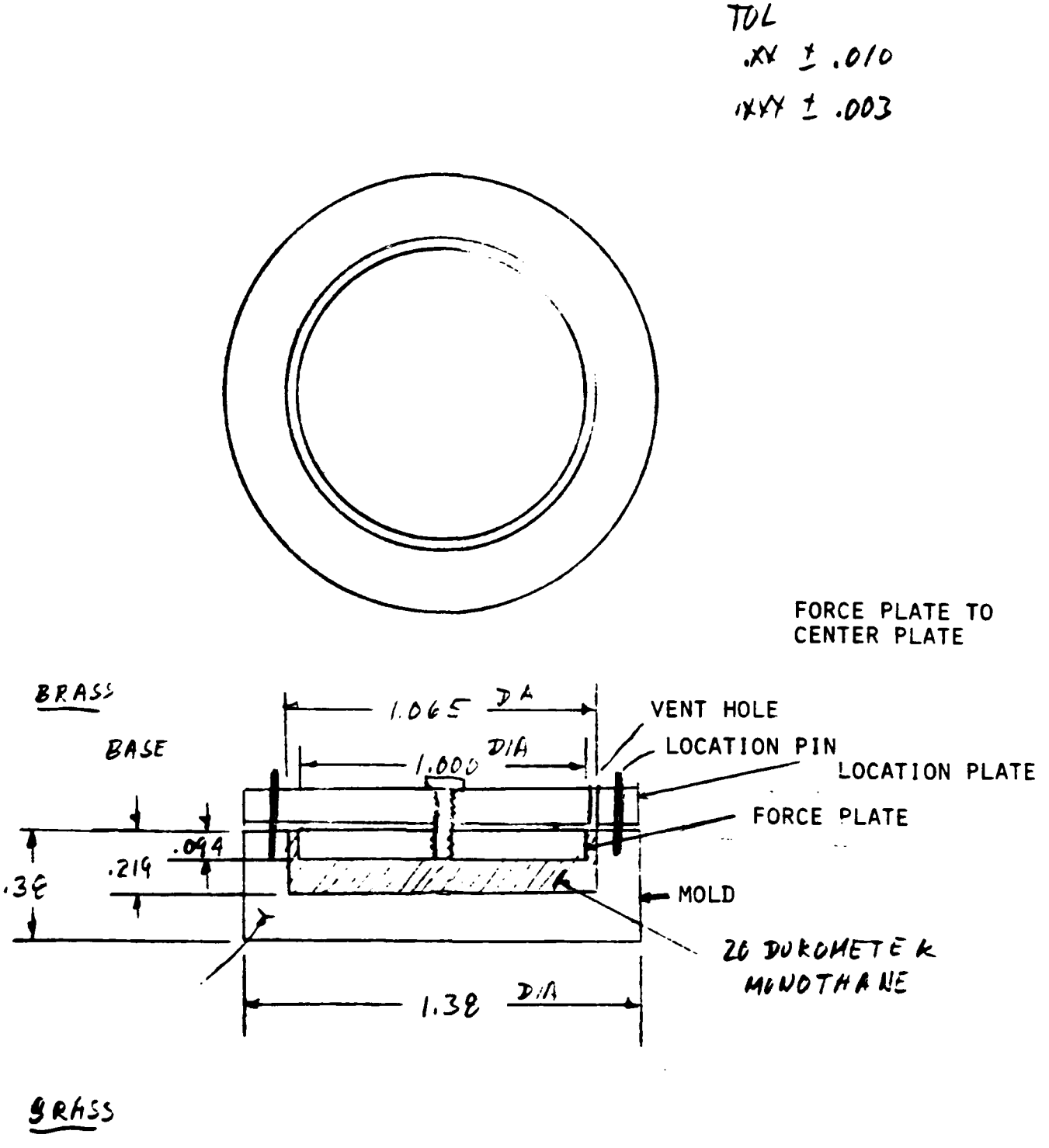

Figure 3.3 Elastomer Mold for One Cell Simulator

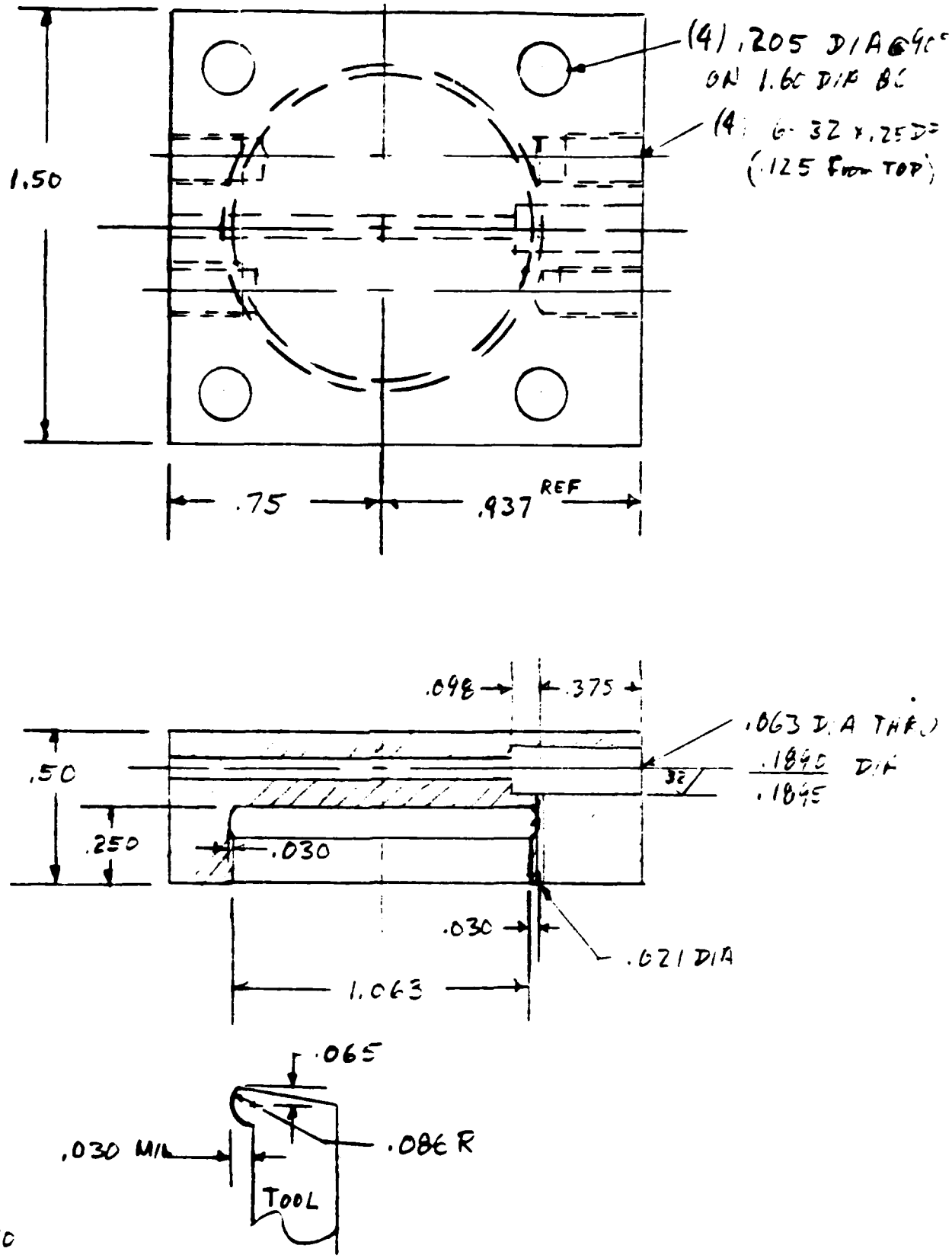

Figure 3.4 One Cell Simulator Compressor

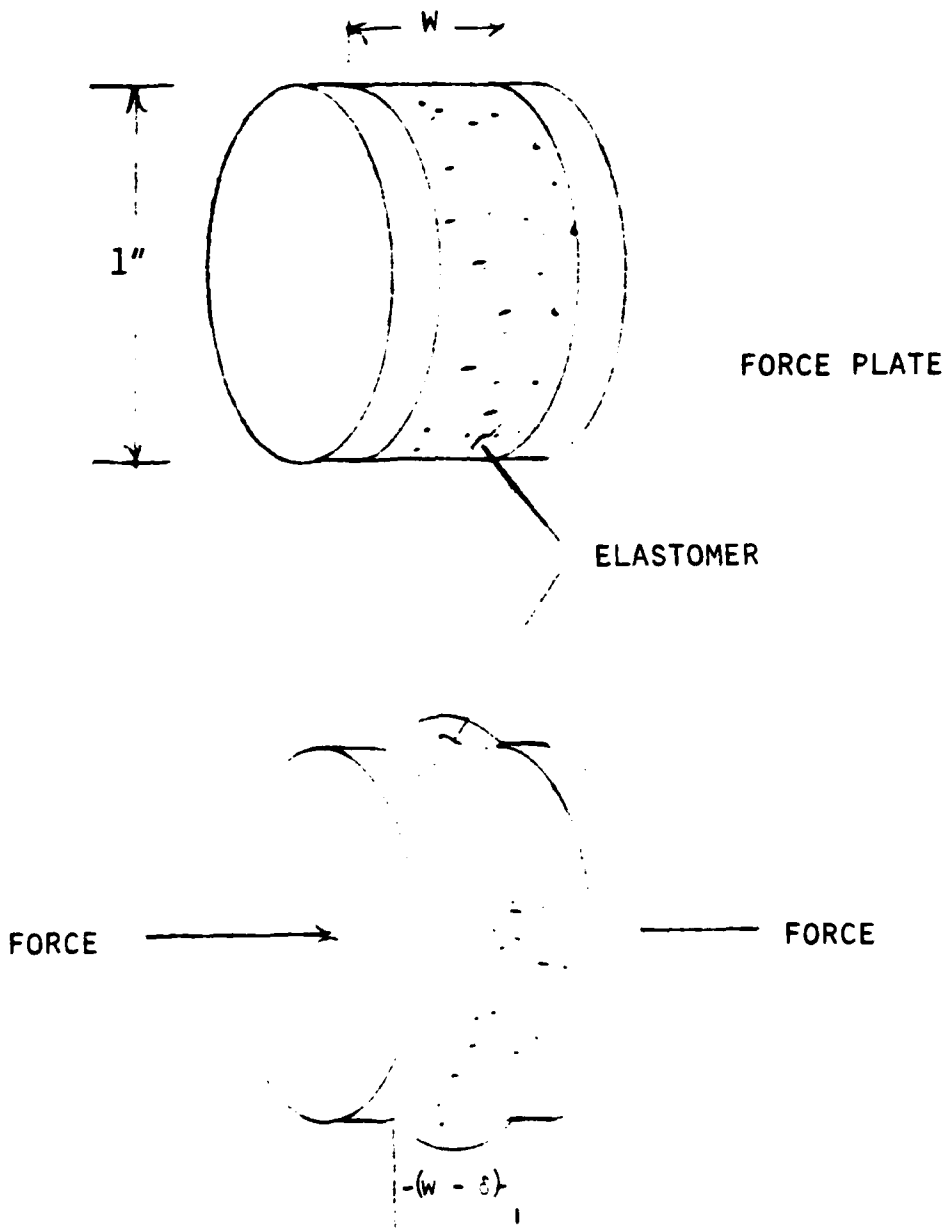

Figure 3.5 Geometry for Elastomer Tests

The elastomer thickness, w, varied from 0.14" to 0.24" in the various elastomers

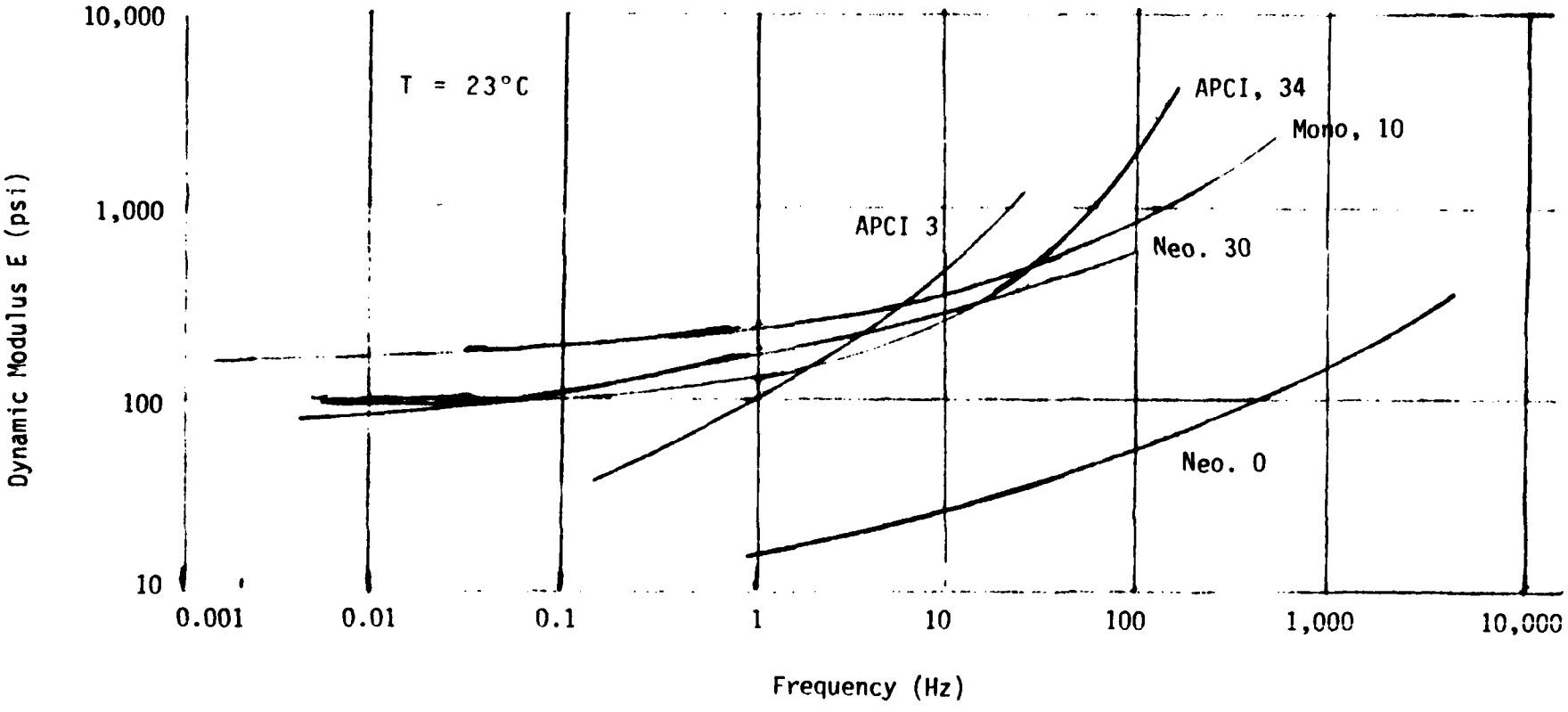

Figure 3.6 Young's Modulus as a Function of Frequency for the Five Elastomers Tested; nominal 10 and 30 Durometer neoprenes and measured 3 and 34 Durometer special Air Products and Chemicals polyurethanes and a 10 Durometer monothane.

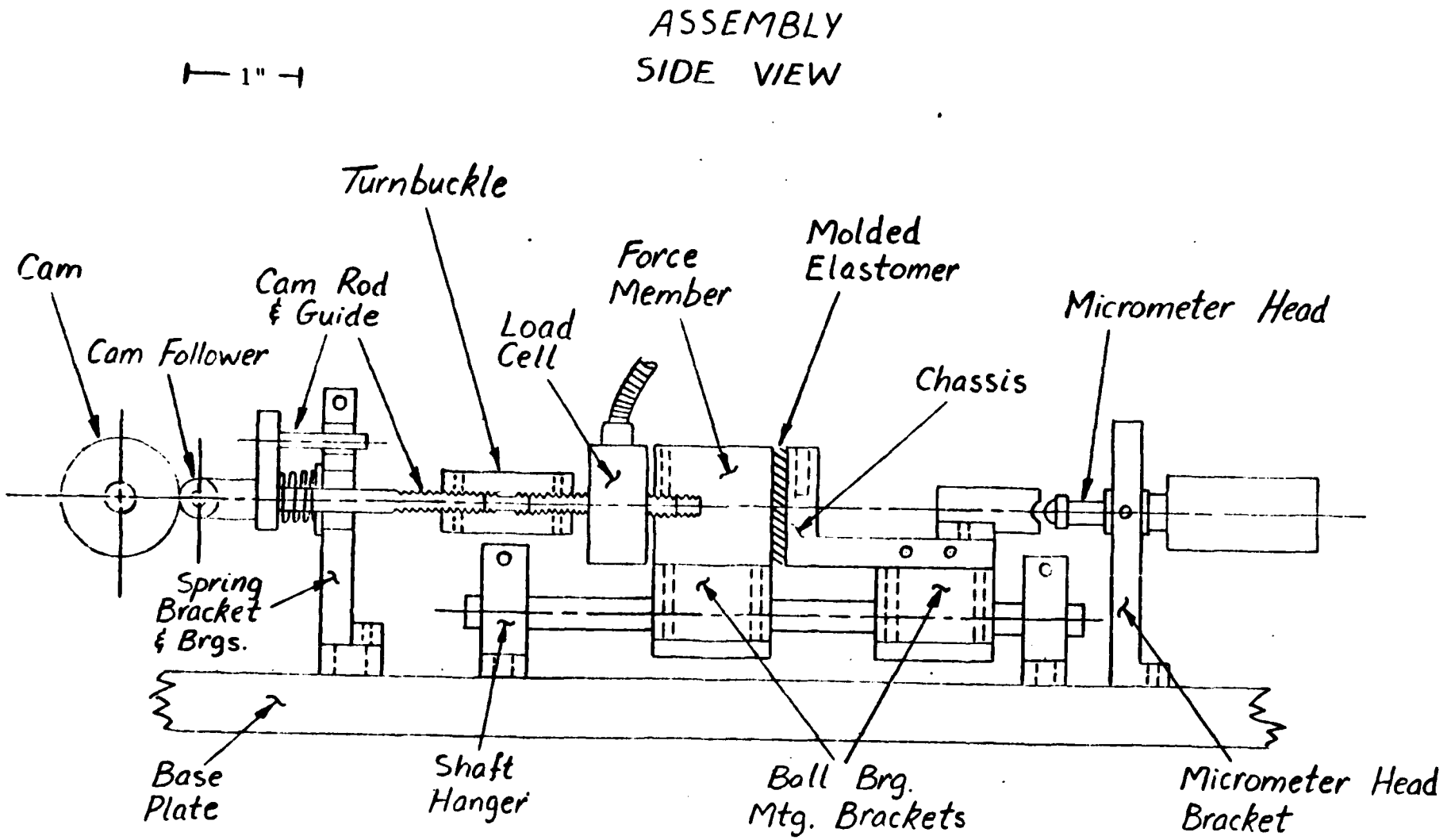

Figure 4.1 Side View of Three Cell Simulator
Shown about 3/4 full scale

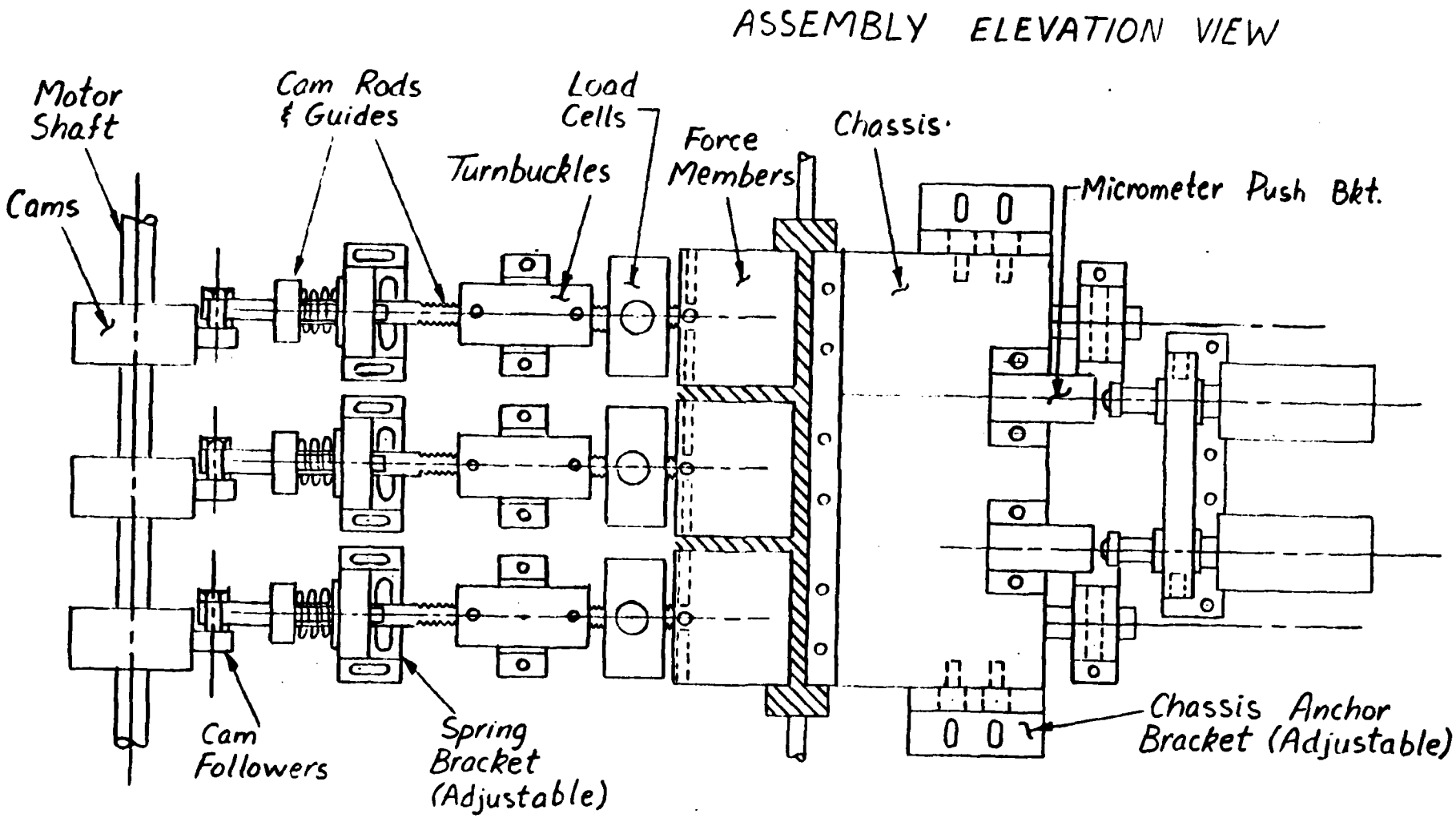

Figure 4.2 Elevation View of Three Cell Simulator
Shown about 3/4 full scale

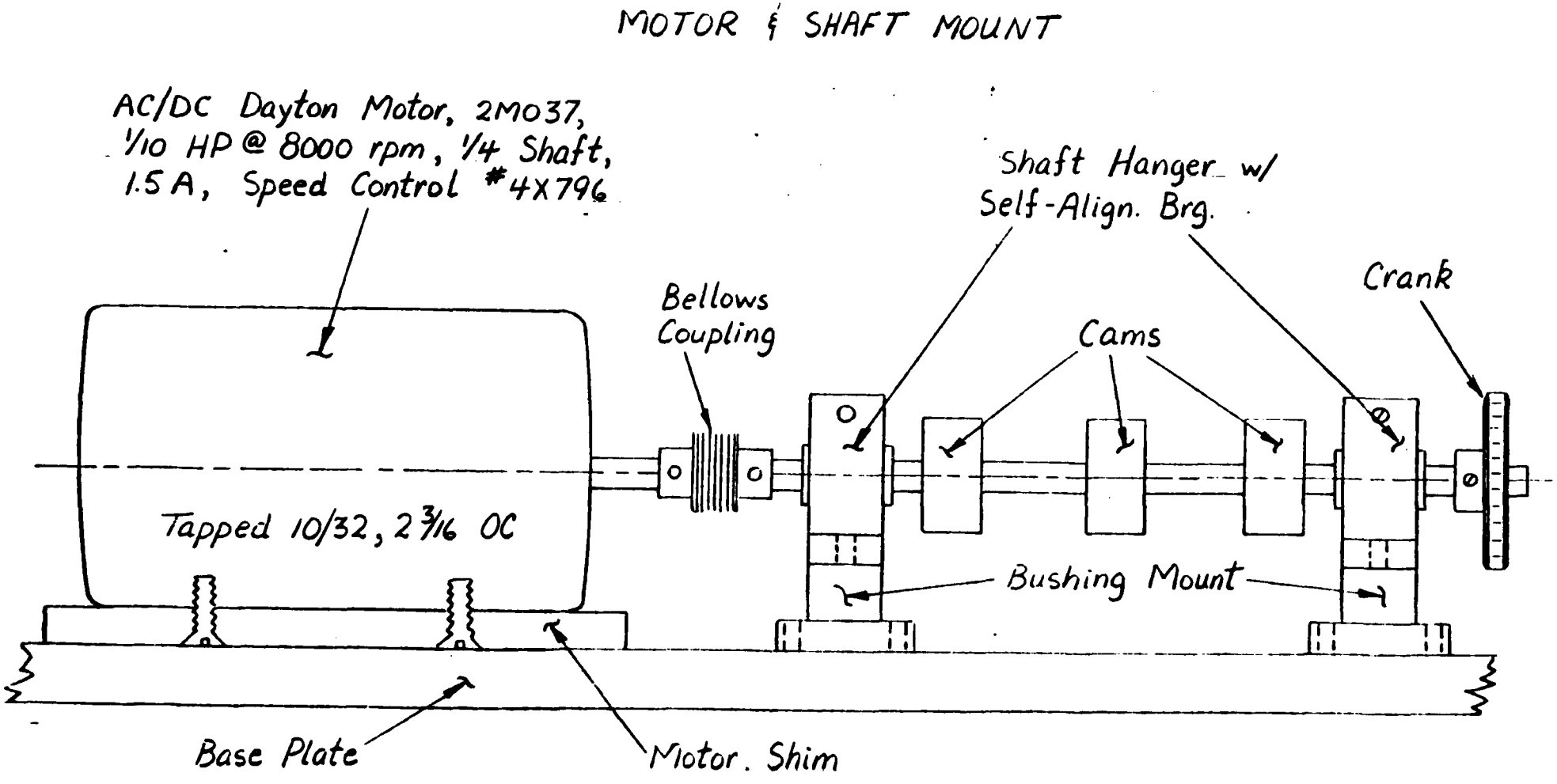

Figure 4.3 End View of Motor, Shaft, and Cam Assembly for Three Cell Simulator
Shown about 3/4 full scale

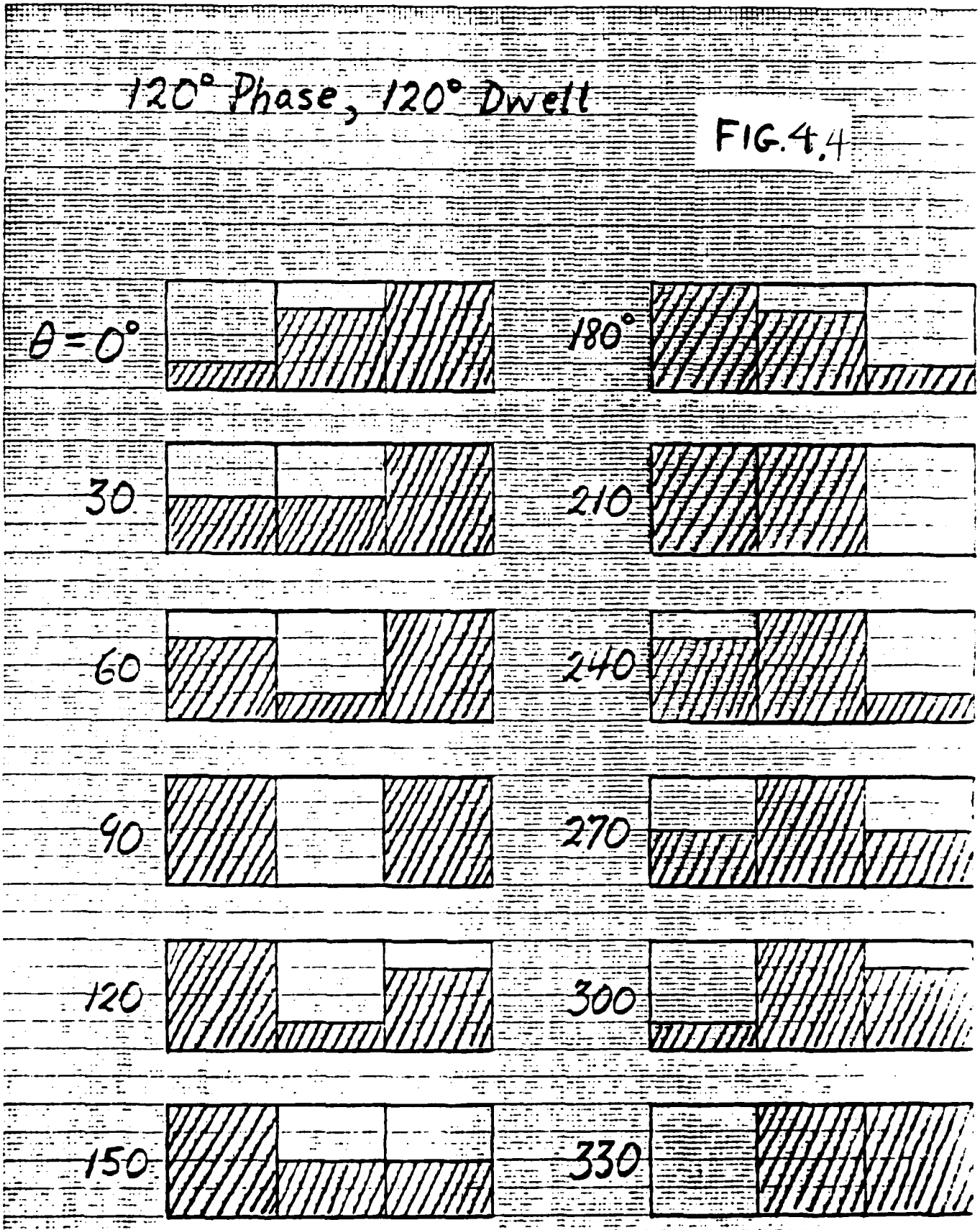

Figure 4.4 Volume of Three Cells in Simulator as a Function of Drive Shaft Angle for 120° Phase and 120° Dwell.

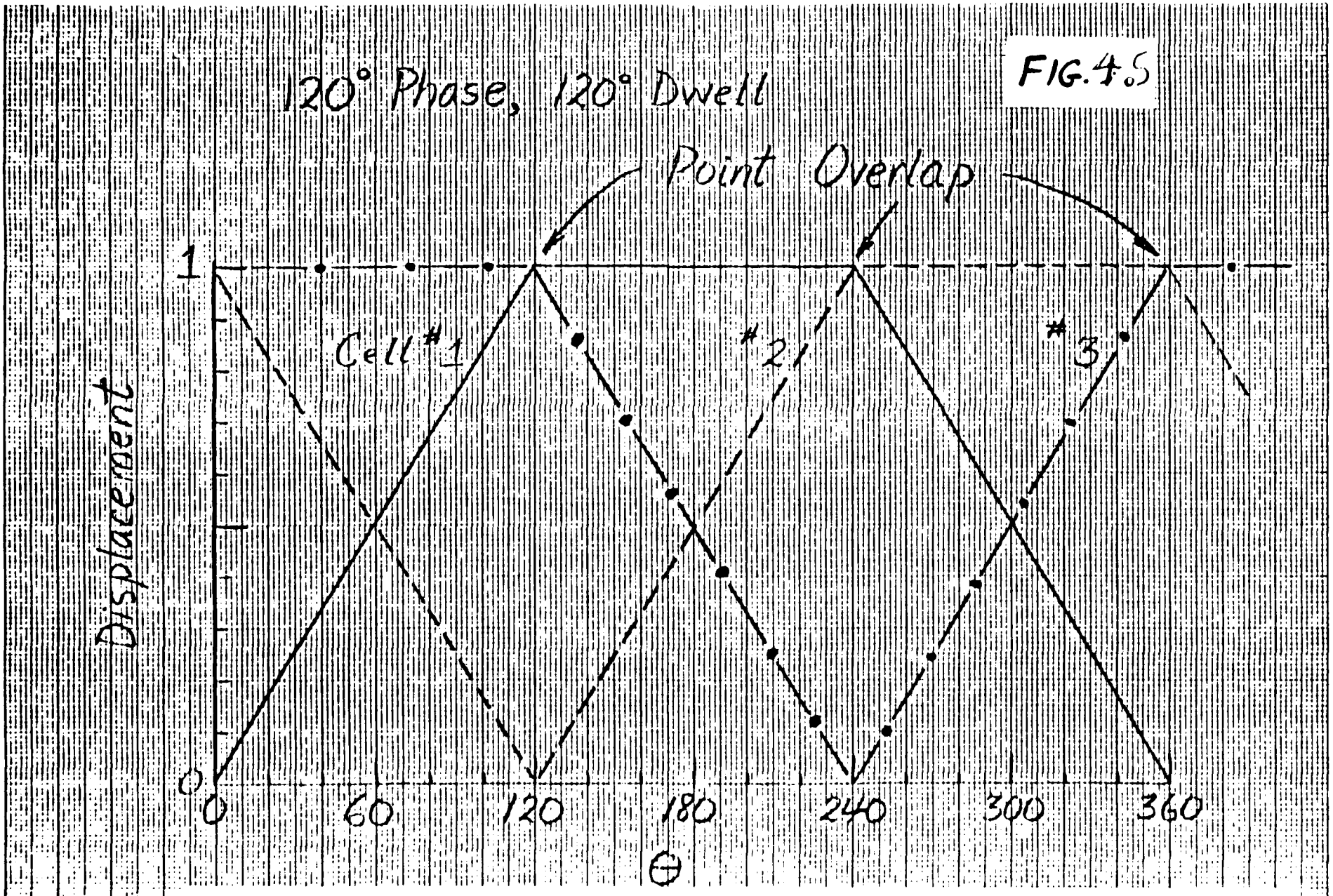

Figure 4.5 Graphic Representation of Elastomer Displacement from Figure 4.4
Cam motion is shown schematically.

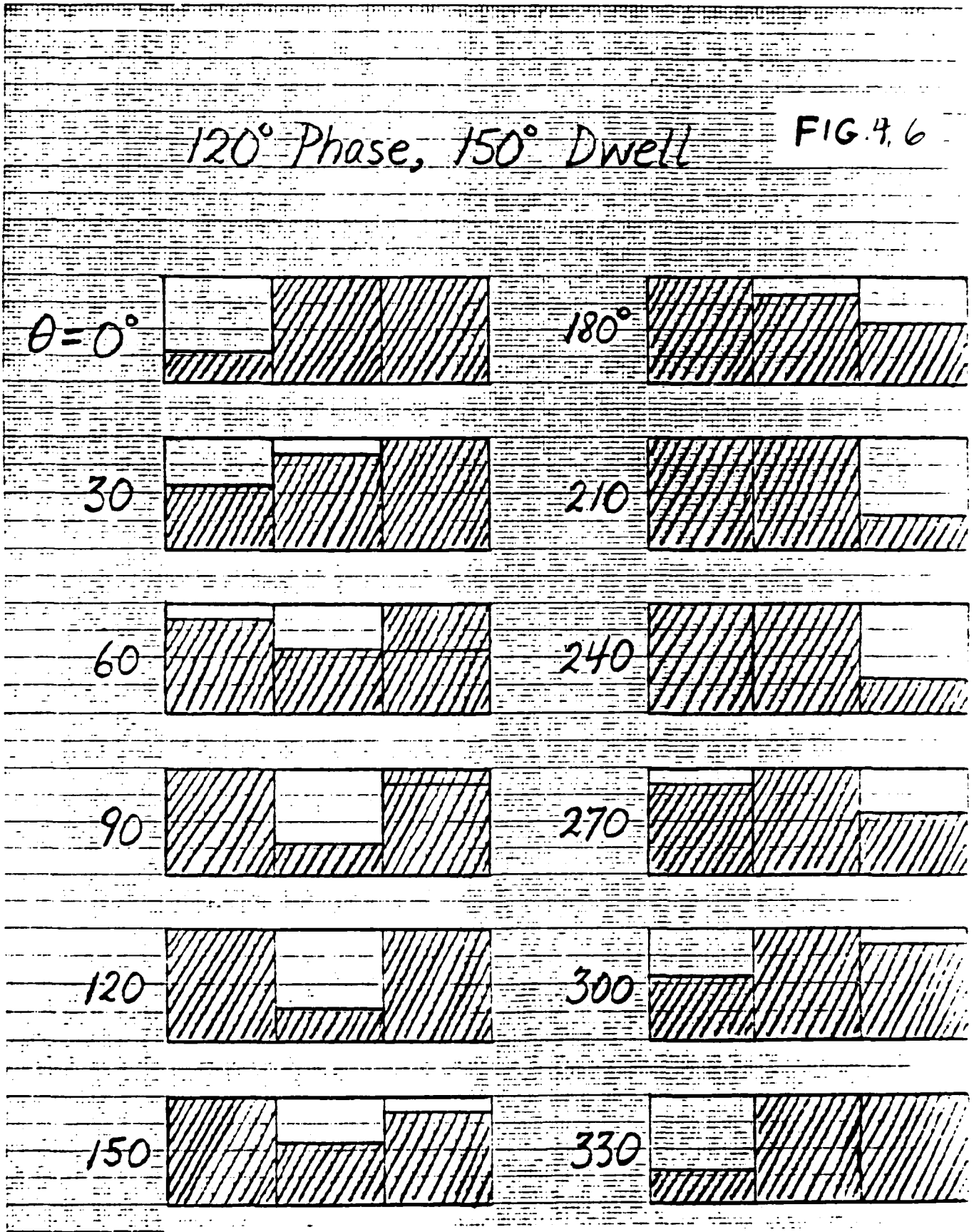

Figure 4.6 Volume of Three Cells in Similar Function of Drive Shaft Angle for 12° Phase and 150° Dwell

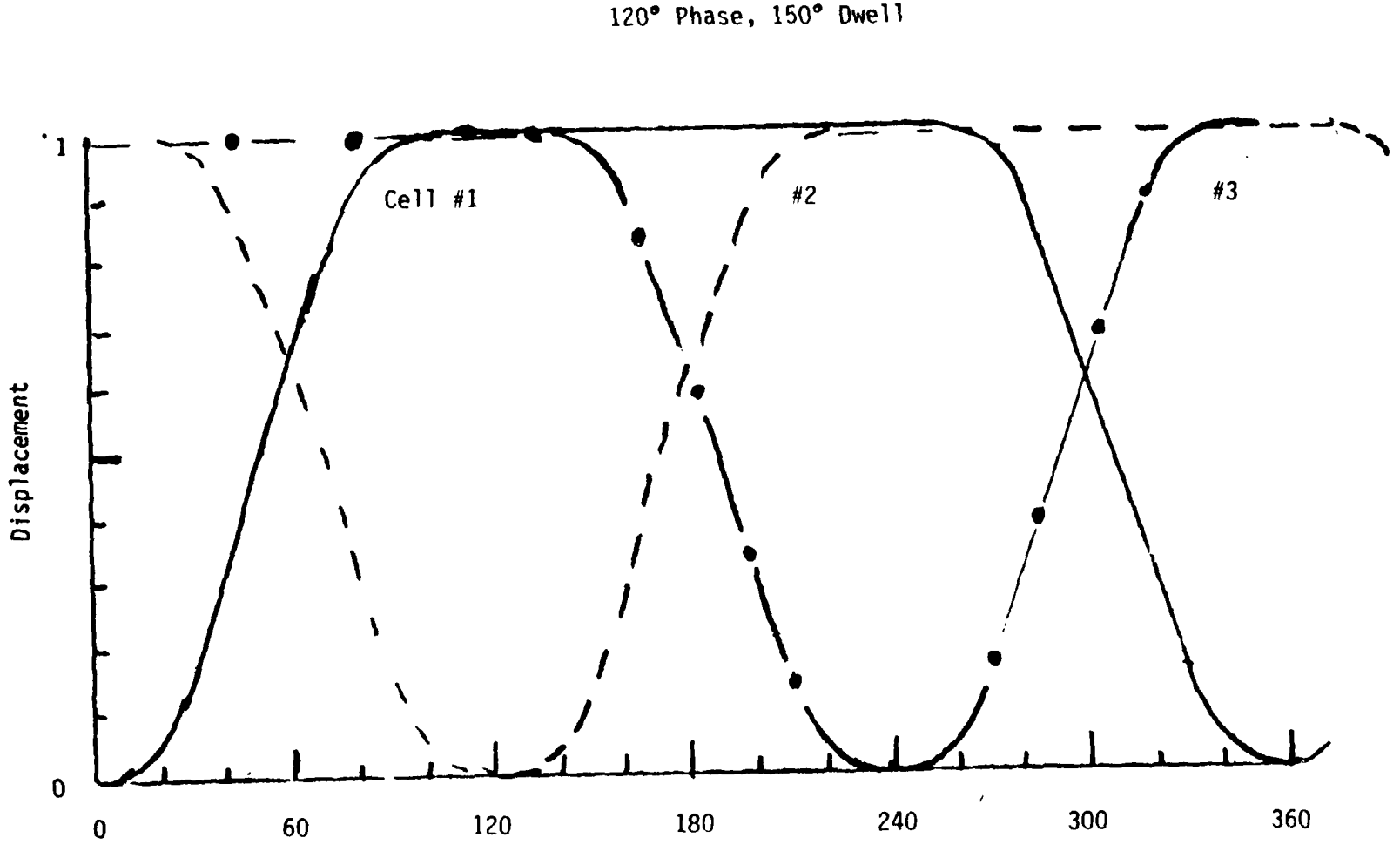

Figure 4.7 Graphic Representation of Elastomer Displacement from Figure 4.6
Cell #1 displacement is given by Eq. 2.

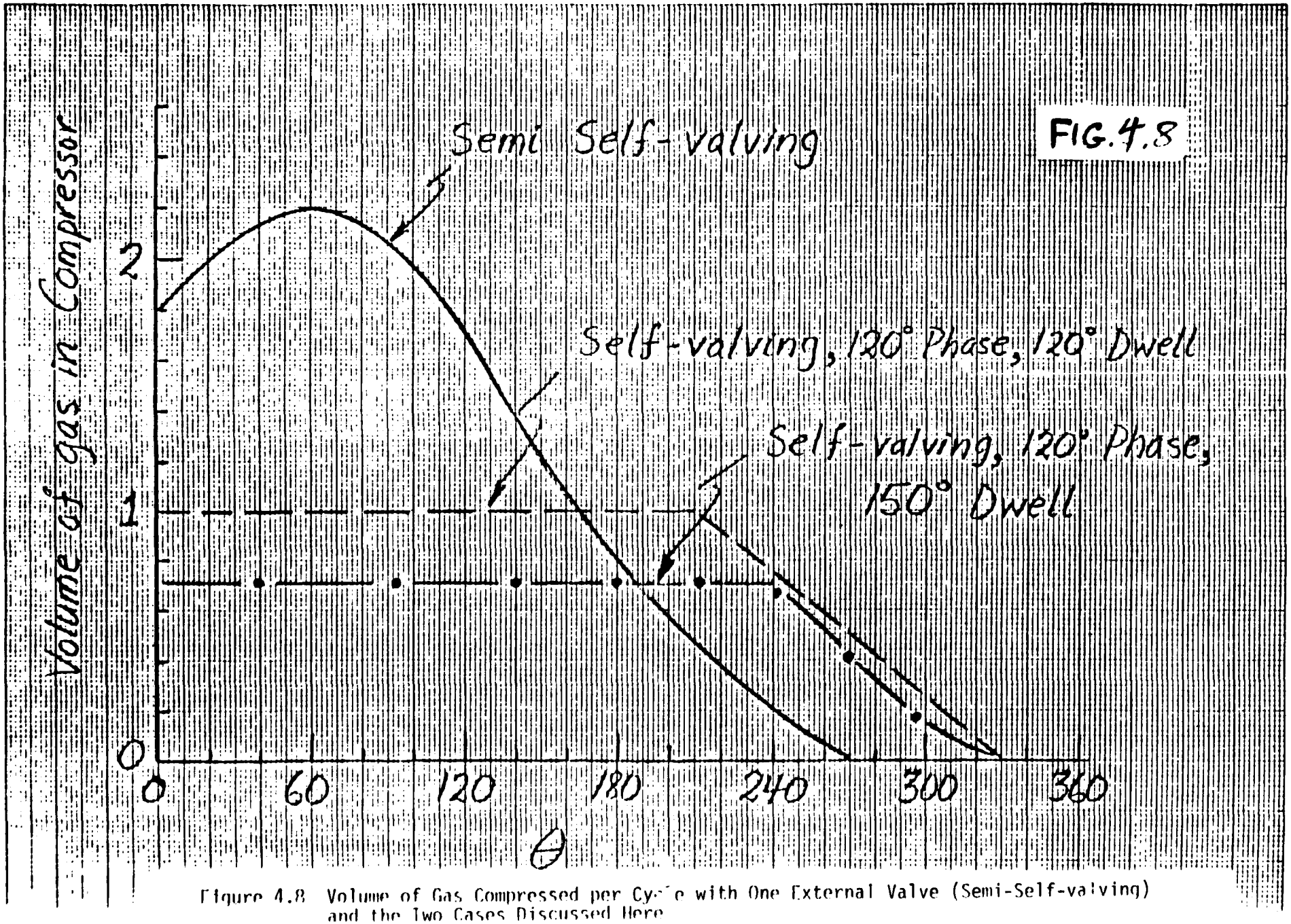

Figure 4.8 Volume of Gas Compressed per Cycle with One External Valve (Semi-Self-valving) and the Two Cases Discussed Here

DARPA TASK SCHEDULE - START 7/1/83

CONTRACT N00014-83-C-0394

	Task	By
1.1	Drivers for Prototype Units	
.1	Develop Type I Ceramics	PSU
.2	Define Design Parameter	PSU
.3	Specify Driver Design	CPI
.4	Fabricate 4 Sets, Deliver	PSU
1.2	Drivers for Final Unit	
.1	Research Type II Ceramics	PSU
.2	Define Design Parameters	PSU
.3	Specify Driver Design	CPI
.4	Fabricate 10 Sets, Deliver	PSU
2.1	One Cell Simulator	
.1	Design One Cell Simulator	APCI
.2	Fabricate One Cell Simulator	APCI
.3	Test Materials	APCI
2.2	Three Cell Simulator	
.1	Design 3 Cell Simulator	CPI
.2	Fabricate 3 Cell Simulator	CPI
.3	Test Pumping Action	CPI
3.	Driver Electronics	
.1	Specify Driver Elec. Charter.	CPI
.2	Design & Fab. Driver Elec./3 Cell	CPI
.3	" " " " /1 Cell	APCI
4.1	System Analysis	
.1	Elastomer Stress, System Design	APCI
.2	Compressor/Driver Analysis	CPI
4.2	Prototype Compressors	
.1	Design, Fab.&Test 1 Cell Proto.	APCI
.2	" " " 3 Cell Proto.	CPI
4.3	Final Compressor	
.1	Design Multicell Compressor	APCI
.2	Fabricate Multicell Compressor	APCI
.3	Test Multicell Compressor	APCI
4.4	Design, Fab. & Test Cryostat	APCI
4.5	Test Final System	APCI
5.1	Status Reports	
.1	Subcontractor Reports, Mo.-15th	PSU
.2	" " " "	CPI
.3	Report to DARPA, Quarterly-30th	APCI
5.2	Interim Technical Reports	
5.3	Final Report	APCI